NUCLEAR SCIENCE AND TECHNIQUES **25**, 020501 (2014)

A method for determination of the *s* orbital component of ^{12}Be ground state*

CAI Xiao-Lu (蔡晓鹭),[1,2,†] FAN Guang-Wei (樊广伟),[3] XU Hang-hua (许杭华),[1,2]
AN Zhen-Dong (安振东),[1,2] FAN Gong-Tao (范功涛),[1] XU Ben-Ji (徐本基),[1]
LI Yong-Jiang (李永江),[1] Pan Qiang-Yan (潘强岩),[4] YAN Zhe (阎喆),[1] and XU Wang (徐望)[1]

[1]*Shanghai Institute of Applied Physics, Chinese Academy of Sciences, Shanghai 201800, China*
[2]*University of Chinese Academy of Sciences, Beijing 100049, China*
[3]*School of Chemical Engineering, Anhui University of Science and Technology, Huainan 232001, China*
[4]*Shanghai Synchrotron Radiation Facility, Chinese Academy of Sciences, Shanghai 201204, China*
(Received January 10, 2014; accepted in revised form March 10, 2014; published online March 20, 2014)

The ambiguity of the structure of ^{12}Be especially in the configuration of ^{12}Be ground state has attracted a lot of attention recently. We notice that the nuclear reaction cross section σ_R at low energy region is sensitive to the surface structure of ^{12}Be, which is greatly impacted by the ground state configuration of ^{12}Be especially by the occupancy probability of the s orbital component. By using existed interaction cross section data of ^{12}Be on C at 790 MeV/nucleon and Glauber model, the upper limit of the s orbital occupation probability of ^{12}Be ground state is roughly determined to be about 56% with Single Particle Model calculations. This demonstrates that the method is very promising to determine the s orbital component of ^{12}Be with proper nuclear-matter density distribution calculations for different orbitals of ^{12}Be ground state. Hence we bring forward to determine the s orbital component of ^{12}Be by measuring the σ_R of ^{12}Be on C and Al at several tens of MeV/nucleon. In this paper, the feasibility and detailed experimental scheme of the σ_R measurement are carefully studied. The precision of the s orbital occupation probability of ^{12}Be ground state is expected to achieve 9% by using the proposed 2% σ_R data.

Keywords: ^{12}Be, Density distribution, MOL[FM], Ground state configuration

DOI: 10.13538/j.1001-8042/nst.25.020501

I. INTRODUCTION

During the past decades, studies on exotic nuclei have been stimulated considerably owing to the enormous development of radioactive ion beam (RIB) technique. Many peculiarities of exotic nuclei have been revealed, such as the halo/skin-like structure [1], the cluster structure [2] and the breakdown of shell closure [3, 4]. Studies on these peculiarities greatly improved understanding of the exotic nuclei, e.g. the beryllium isotopes. Theoretical researches on properties of Be isotopes are based on the three-body model [5, 6] and the density-dependent relativistic mean-field model [7, 8]. The neutron halo of ^{14}Be has been well explained using these models [5–8]. Located between the halo nuclei ^{11}Be and ^{14}Be, ^{12}Be is an interesting combination of the peculiarities and plays a key role in the beryllium chain. In shell model, ^{12}Be is supposed to be a "magic nucleus" with simple structure. But recent experiments [4, 9, 10] provided direct evidence for breakdown of the $N = 8$ shell closure in ^{12}Be and the (s, d) intruder states. In principle this intruder-state configuration can cause halo-like structure, yet neither the wide momentum distribution [11] nor the relative large two-neutron separation energy ($S_{2n} = 3.67$ MeV [12]) indicates the signature for a halo. There exists controversy between the recent theoretical and experimental results on halo-like structure of ^{12}Be. The giant deformation in the ground state of ^{12}Be [13] is also predicted by Antisymmetrized Molecular Dynamics (AMD), the ground state structure of ^{12}Be is still ambiguous. Also, explorations in the level structure, parity, spin and deformation of the excited states of ^{12}Be with molecular cluster model draws quite a lot of attentions [14–18]. The ground state structure properties of ^{12}Be are indispensable in the studies because it provides fundamental information for the studies of the excited states. Therefore, it is of significance to study the ground state structure of ^{12}Be.

As an essential property of the ground state structure, the nuclear-matter density distribution of ^{12}Be not only provides basic structure information such as nuclear-matter radius, but also helps to determine whether the ^{12}Be ground state has a halo structure. Recently, particle-particle random-phase approximation (pp-RPA) [19] and microscopic no-core shell-model (NCSM) calculations [18] have shown that the ground state wave functions of ^{12}Be are dominated by the p shell configuration, which is in conflict with the previous calculations [20–24] and the knockout measurements [4, 9]. The nuclear-matter density distribution may be used to determine the configuration mixing between the $1p_{1/2}$, $1d_{5/2}$ and $2s_{1/2}$ orbitals, thereby help to resolve the inconsistencies between current data and various theoretical models. Therefore, we were motivated to determine the nuclear-matter density distribution of ^{12}Be ground state.

In the following text, the experimental method of the σ_R measurement is introduced in Sec.II, the feasibility analysis and optimization of the reaction cross section (σ_R) measurement are elaborated in Sec.III, the way to determine the s orbital component of ^{12}Be ground state through σ_R is illustrated in Sec.IV, and a summary is given in Sec.V.

* Supported by the National Natural Science Foundation of China (No. 11179018 and 11305238) and the Instrument Developing Project of the Chinese Academy of Sciences (No. YZ201246)
† Corresponding author, caixiaolu@sinap.ac.cn

II. GENERAL SCHEME

Typically the nuclear-matter density distribution is investigated by measuring the σ_R (or the total interaction cross sections σ_I). This involves theoretical models, and several methods were developed to study the total reaction cross section, such as the multi-step scattering theory of Glauber [25], the transport model method of Ma *et al*. [26, 27] and the semi-empirical formula of Kox *et al*. [28] and Shen *et al*. [29] A series of investigations to ^{12}Be were carried out in the past decades. By measuring the σ_I on Be, C and Al at 790 MeV/nucleon, Tanihata *et al.* successfully determined the effective root-mean-square (RMS) radius of ^{12}Be through a Glauber model in 1988 [30]. Liatard *et al.* measured the σ_R of radioactive Be isotopes on Cu at around 25 to 65 MeV/nucleon and deduced the radii by using a simple microscopic model [31]. Later, Warner *et al.* measured the σ_R of ^{12}Be on Pb and Si at about 30 to 60 MeV/nucleon and obtained the radius of ^{12}Be [32]. However, the studies have several drawbacks. First, their energy region did not cover both low and high energy regions. Data at low energy region give constraint to the outer structure, and data at high energy region provide more information on the core part, hence low and high energy region data are both needed to obtain accurate nuclear-matter density distribution. Second, generally, their targets were too heavy. This makes σ_R insensitive to the surface structure of ^{12}Be. Third, their models were too simple to interpret the data especially at low energies. The results did not give detailed nuclear-matter density distribution of ^{12}Be especially for the surface area.

In obtaining detailed outer structure of the nuclei, two improvements were made recently for extracting accurate nuclear-matter density distribution of nuclei. First, the method of proton elastic scattering at intermediate energies was developed. Ilieva *et al*. applied proton-scattering method in 2012 to ^{12}Be [33] and determined the nuclear-matter density distribution of ^{12}Be ground state. But the result has considerable uncertainty because of various parametrizations. So the method is not well established yet for studing the surface structure of especially unstable nuclei. Second, the applicability of Glauber model in the whole energy region was studied and a Modified Optical Limit Glauber model (MOL[FM]) was developed by incorporating the Fermi motion of nucleons in the finite-range MOL [34]. The MOL[FM] has reduced the discrepancy between the data of calculation and measurement to just 1%–2% for the whole energy region. By measuring the σ_R on Be, C and Al targets at intermediate energies, the nuclear-matter density distributions of ^{22}C [35] and ^{17}Ne [36] were determined accurately with MOL[FM]. Through this method we obtained the nuclear-matter density distribution of ^{8}Li [37] precisely and the relevant paper about our further study is in preparation. Therefore, MOL[FM] provides a powerful tool for interpreting the σ_I or σ_R data, and measuring the σ_I or σ_R determining the nuclear-matter density distribution with MOL[FM] is still a good method at present.

Thus, we were motivated to precisely measure σ_R of ^{12}Be at low energy region and extract the nuclear-matter density distribution of ^{12}Be ground state using MOL[FM].

Refer to the measurements of σ_R, transmission method is usually used. Typical experimental procedures are given in Ref. [38]. The σ_R is obtained by Eq. (1),

$$\sigma_R(E) = -\frac{1}{t}\ln R, \tag{1}$$

where E is the energy point; t is the target thickness expressed by the target particles numbers per unit area; and $R = N_{\text{out}}/N_{\text{in}}$ is the ratio of outgoing projectile particles number to incident projectile particles. Since energy of the projectile particles decreases as passing through the target, we determine the energy point of σ_R by mean energy E_{mean}, which is given by

$$E_{\text{mean}} = \int_0^t \frac{E(x)}{t}\mathrm{d}x, \tag{2}$$

where t is the target thickness, and $E(x)$ is the residual energy of incident beam travelling along the path by distance x. $E(x)$ can be calculated by the improved Bethe-Bloch formula [39].

The main relative error of σ_R can be written as

$$\left(\frac{\Delta\sigma_R}{\sigma_R}\right)^2 = \left(\frac{\Delta t}{t}\right)^2 + \left(\frac{1}{\ln R}\right)^2 \left[\left(\frac{\Delta R}{R}\right)^2_{\text{sys}} + \left(\frac{\Delta R}{R}\right)^2_{\text{stat}}\right], \tag{3}$$

where $\Delta t/t$ stands for uncertainty of the target thickness, the subscripts "sys" and "stat" denote the systematic and statistical error of R, respectively, and the statistical error of R is given by

$$\left(\frac{\Delta\sigma_R}{\sigma_R}\right)_{\text{stat}} = \sqrt{\frac{1-R}{N_{\text{in}}R}}, \tag{4}$$

because it follows the binomial distribution. In practice, $R_{\text{in}}/R_{\text{out}}$ is taken as R in order to remove the events interact outside the target, R_{in} and R_{out} are the ratios of $N_{\text{out}}/N_{\text{in}}$ corresponding to the target-in and target-out measurements, respectively. Accordingly, the relative error of σ_R becomes

$$\left(\frac{\Delta\sigma_R}{\sigma_R}\right)^2 = \left(\frac{\Delta t}{t}\right)^2 + \left(\frac{1}{\ln R}\right)^2 \left(\frac{\Delta R}{R}\right)^2_{\text{sys}} + \frac{1}{\sigma_R^2 t^2}\left(\frac{1-R_{\text{in}}}{N_{\text{in}}^{\text{tar-in}}R_{out}} + \frac{1-R_{\text{out}}}{N_{\text{in}}^{\text{tar-out}}R_{\text{out}}}\right). \tag{5}$$

Besides the contribution of statistical error, the systemic uncertainty of σ_R is mainly from the correction of the num-

ber of inelastic-scattering events merged into the non-reaction events. By using the method in Ref. [40] and Monte Carlo simulation, the systematic error of σ_R can be limited within 1%–2% [34]. So 1%–2% total uncertainty can be achieved if sufficient reaction events are recorded. In fact, this was achieved recently in most experiments of the kind.

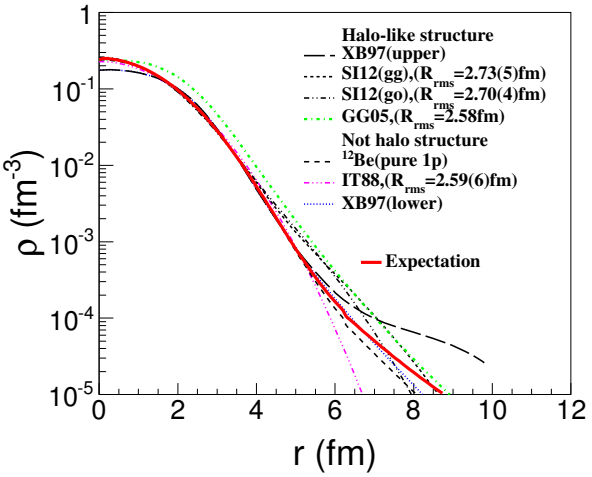

Fig. 1. (Color online) Current results of the nuclear-matter density distributions of ^{12}Be (XB97: [41], SI12: [33], GG05: [42], IT88: [30]). The solid line is given by the sum of the nuclear-matter density distribution of ^{10}Be core in ref. [33] and that of two valence neutrons calculated in section 4 with the configuration in ref. [4].

Based on available nuclear-matter density distributions of ^{12}Be from experiments and theories (Fig. 1), we calculated the σ_R (Fig. 2) at different energies by MOL[FM]. The momentum width and the finite-range parameter β were taken from Ref. [34]. From Fig. 2 one sees that below $\sim$50 MeV/nucleon, σ_R data with uncertainty around 2% is sufficient to distinguish several previous results and determine whether ^{12}Be has a clear halo-like structure.

However, the specific requirement on experimental conditions for a 2% precision of σ_R is still unknown, and investigation is needed for further discussion of the method's feasibility.

III. FEASIBILITY STUDY AND OPTIMIZATION OF σ_R MEASUREMENT

To make sure that the experiment is practical, we have studied the feasibility and optimized the experimental method. The experiment feasibility mainly relies on detecting system, reaction targets and ^{12}Be beam. In the energy region below 50 MeV/nucleon, $\Delta E - E$ method is often used for particle identification. The required energy deposition of ^{12}Be in the ΔE detector is about 10 MeV/nucleon, while the required energy in the E detector shall be above 10 MeV/nucleon, just for ensuring validity of the particle identification. So the energy of ^{12}Be right before the ΔE detector is supposed to be over 20 MeV/nucleon. Usually Si detector and scintillator detector

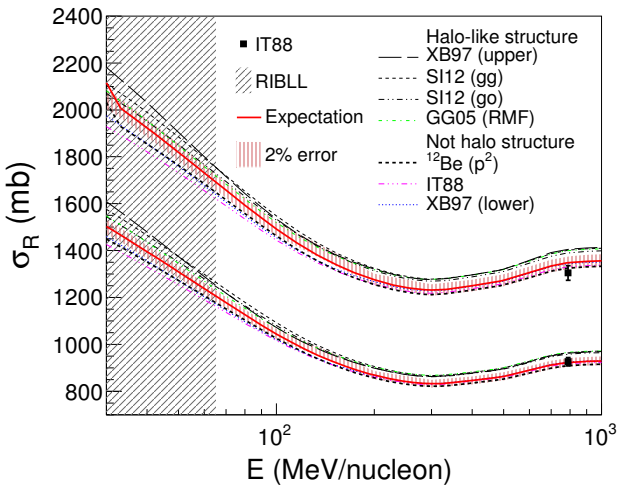

Fig. 2. (Color online) The calculations of $\sigma_R(E)$ corresponds to current nuclear-matter density distributions of ^{12}Be (XB97: [41], SI12: [33], GG05: [42], IT88: [30]). The upper group of lines corresponds to the σ_R of ^{12}Be + Al, and the lower group of lines corresponds to the σ_R of ^{12}Be + C.

are used as the ΔE and E detector, respectively. Their thicknesses depend on the specific energy of ^{12}Be right before the ΔE detector. As for the particle identification before the reaction target, $B\rho$-ΔE-TOF technique is often used. Typical layout of the detecting system is shown in Fig. 3.

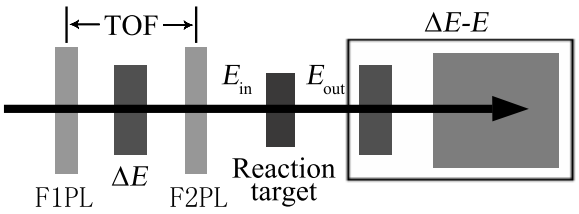

Fig. 3. Schematic diagram of typical experimental setup.

Besides the detection system, the target material and thickness t and incident energy of the ^{12}Be beam E_{in} shall be determined before the experiment. Regarding the target material, ^{12}C is a good candidate, because its nuclear-matter density distribution is well determined and its mass number is comparable with ^{12}Be, so its σ_R is more sensitive to the ^{12}Be surface structure. Another target, ^{27}Al, is also needed for reducing the target-dependence of the result.

For the t and E_{in}, there are direct impact factors, such as the transmission rate R, ^{12}Be outgoing energy E_{out} after the reaction target, and energy point E_{mean} with certain restriction for each of these factors, hence it is difficult to consider t and E_{in} separately. We studied the relations between these parameters through calculations, which includes:

(1) E_{out} for certain E_{in} and t, E_{out} was calculated by LISE++ [43];

(2) E_{mean} could be determined through (E_{in} + E_{out})/2 ap-

proximately;

(3) $\sigma_R(E_{\rm mean})$ was calculated using MOL[FM] based on the nuclear-matter density distribution of the expectation in Fig. 1;

(4) R is calculated by Eq. (1) with certain t and corresponding $\sigma_R(E_{\rm mean})$.

Then, the trends of R varying with $E_{\rm in}$ under different t and E_{out} were obtained. Fig. 4 shows the calculation results of ^{12}Be+C. Each dash line corresponds to the same t, each dash dot line corresponds to the same $E_{\rm out}$. Subsequently, we took into account the restrictions of R, $E_{\rm out}$ and $E_{\rm mean}$ to give proper t and $E_{\rm in}$. As mentioned before, $E_{\rm mean}$ should be less than 50 MeV/n to ensure the physical goal, and $E_{\rm out}$ (viz. the energy of ^{12}Be right before the ΔE detector) should be above 20 MeV/n to ensure the availability of $\Delta E - E$ method.

R is restricted by systematic error if the statistical error is small enough. It is of certain difficulty to achieve 0.1% systematic error for a directly measured quantity, like R. To ensure a $< 2.5\%$ precision of σ_R, the factor $1/\ln R$ before the systematic error of R in Eq. (5) shall be less than 25. Accordingly R should be less than 0.96. Therefore, proper ranges of t and $E_{\rm in}$ are indicated as the hatched area in Fig. 4.

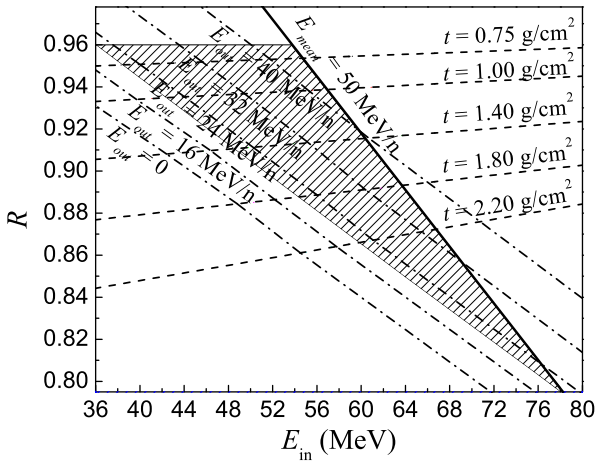

Fig. 4. The change trends of R with $E_{\rm in}$ under different t and $E_{\rm out}$.

In the energy region of 30–50 MeV/nucleon we intend to obtain three data points by using subtraction method. As shown by Conditions (1) and (2) in Fig. 5, at incident beam energy of E_1 and E_2, with target thickness of t_1 and t_2, reaction cross sections σ_1 and σ_2 are measured by the transmission method, respectively, and by adjusting E_1 and E_2, both the outgoing beam energies $E_{\rm out}$ can be of the same energy. Then, the reaction rate in the target in Condition (2) shall be equal to that of the corresponding thickness of t_2 in the target in Condition (1). By subtracting the two data, one obtains another σ_R as,

$$\sigma_R^{\rm sub} = \frac{-1}{t_1 - t_2} \ln\left(\frac{R_{\rm in-1}}{R_{\rm in-2}}\right) = \frac{1}{t_1 - t_2}(t_1\sigma_1 - t_2\sigma_2), \quad (6)$$

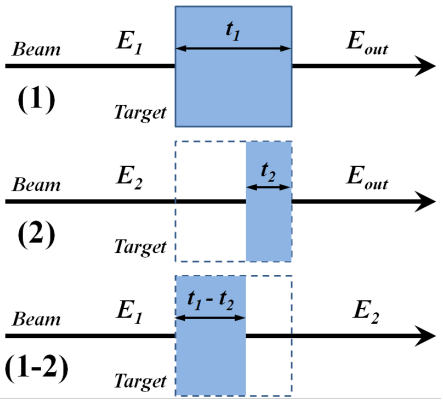

Fig. 5. (Color online) Schematic diagram of the subtraction method.

where $R_{\rm in-1}$ and $R_{\rm in-2}$ denote the transmission rates of the target-in experiment in Conditions (1) and (2), respectively. The transmission rates of the target-out experiments do not appear in Eq. (6) because the reaction rate outside the target is canceled between the two measurements. The error of this deduced σ_R was determined in Ref. [40]. Through this method, three data points can be obtained with only two measurements. This greatly improves the efficiency of the experiment. The key point is that the outgoing energies $E_{\rm out}$ in the two measurements should be the same. And the interval between the two adjacent incident beam energies $E_{\rm in}$ should be over 15 MeV/nucleon in order to make sure the energy points are evenly distributed between 30–50 MeV/nucleon.

Thus we have decided the range at $E_{\rm in}$, and C and Al target thicknesses, and the detecting system. Next, we are to determine the number of events we need according to the requirement of the statistical error, and estimate the requisite beam intensity.

According to Eq. (3) the statistical error should be less than 0.5%, so that it will not be a main error source, which gives

$$\frac{1}{|\ln R|}\sqrt{\frac{1-R}{R}}\frac{1}{\sqrt{N_{\rm in}}} < 0.5\%. \quad (7)$$

Since R is at most 0.96, $N_{\rm in}$ of 10^6 is already sufficient. So, it will take only 10^3 seconds of beam time under typical condition of 10^3 s^{-1} beam intensity, which is very practical.

TABLE 1. Experimental scheme

Beam	$E_{\rm in}$ (MeV/n)	$E_{\rm out}$ (MeV/n)	Target	Thickness (g/cm^2)	R	$N_{\rm in}$
^{12}Be	62.7	24	C	2.33	0.86	2.9×10^5
			Al	2.70	0.90	4.0×10^5
	42.4	24	C	0.90	0.94	6.7×10^5
			Al	1.05	0.96	1.0×10^6

To sum up, for the experiment a ^{12}Be beam of about 10^3 s^{-1} intensity at 20–70 MeV/nucleon is needed to provide the projectile particles, and the outgoing energy of ^{12}Be after the reaction targets in the two measurements should be the same. In addition, a Si and a scintillator detector are

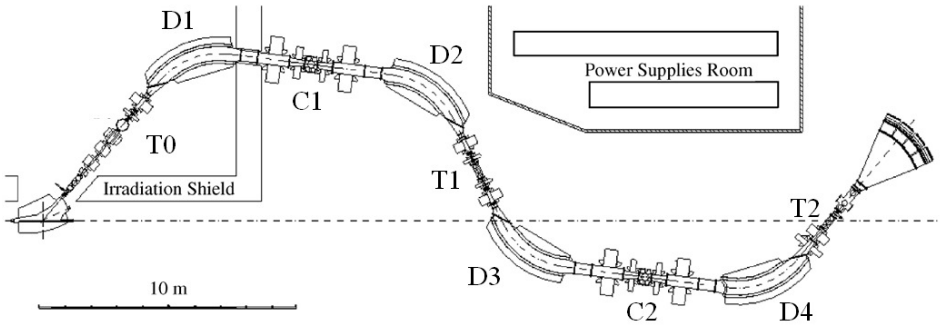

Fig. 6. Schematic diagram of the layout of RIBLL.

needed for particle identification. Finally, we select two energy points, find the corresponding target thickness, evaluate the R and decide corresponding requirement of $N_{\rm in}$. The detailed experimental scheme is given in Table 1.

We find that the Radioactive Ion Beam Line in Lanzhou (RIBLL) [44] is a suitable candidate for providing ^{12}Be beam. The schematic diagram of the layout of RIBLL is shown in Fig. 6.

The primary beam $^{18}O^{8+}$ is accelerated by the Heavy Ion Research Facility of Lanzhou (HIRFL) and introduced to RIBLL. It bombards the production target of Be at T0 and generates the secondary beam of ^{12}Be. An Al degrader at C1 is used for an energy-loss analysis of the secondary beam separation. Another Al degrader at T1 is used for energy degradation. Two slits at C1 and C2 is used for momentum acceptance controlling. Two plastic scintillation counters at focal points T1 and T2 can provide the TOF information. Si solid state detector (SSD) at T2 can be used to provide the ΔE signals for particle identification before the reaction target. Energy $E_{\rm in}$ of the incident beam right before the reaction target is determined by the $B\rho$ value of the fourth dipole magnet D4. Based on this configuration, the ^{12}Be beam condition is simulated by LISE++ using a typical 100 enA primary beam of $^{18}O^{8+}$ at 80 MeV/nucleon. Major parameters of the simulation result given in Table 2. It's worth mentioning that similar experiments have been performed on RIBLL since 2000 [45–49]. From their results we infer that typically the error of σ_R is up to about 5% including 3%–4% systematic error. So we need further consideration based on the real performance of RIBLL to reduce the error especially the systematic error.

For the detecting system, typically a Si detectors of 1500 μm thickness is competent for the ΔE measurement, and a CsI(Tl) scintillator detector of 30 mm thickness is adequate for the E measurement. It should be noted that the Si detector is made of single crystal, hence the concern of channeling effect to the particles being detected. By tilting the Si detector against the beam axis at a certain angle, the fraction of channeling events can be reduced to $< 1\%$ [40]. The tilting angle can be determined by studying the angle dependence of the channeling events in advance.

Based on the above feasibility study, the σ_R measurement is reasonable and valid, and the requisite conditions can be satisfied. Through the measurement the nuclear-matter density distribution of ^{12}Be ground state can be determined and then used to extract the component of ^{12}Be ground state. In Sec.IV, we elaborate that how to determine the s orbital component through σ_R.

TABLE 2. Major parameters of ^{12}Be beam condition at RIBLL

Items[a]	Value 1	Value 2	Value 3
Production target thickness (mg/cm^2)	370	740	740
D1 (Tm)	3.7594	3.5621	3.4911
C1 degrader[b] thickness (mg/cm^2)	810	1350	1350
D2 (Tm)	3.5355	3.1014	3.0010
T1 degrader[b] thickness (mg/cm^2)	0	540	1350
D3 (Tm)	3.5335	2.8575	2.1478
D4 (Tm)	3.5335	2.8575	2.1478
Beam energy (MeV/nucleon)	62.73	42.42	24.06
Beam rate (s^{-1})	3940	3140	789
Beam purity	99.1%	99.3%	98.9%

[a] The C1 slits are of 40 mm (H), and the C2 slits are of 40 mm × 140 mm (H×V).
[b] The degrader is plane-shaped.

IV. EXTRACTION OF THE s ORBITAL COMPONENT OF ^{12}BE GROUND STATE

As shown by the fermionic molecular dynamics (FMD) calculations (see the inset (b) in Fig. 10 of Ref. [33]), different configuration mixings of the two valence neutrons in ^{12}Be lead to different nuclear-matter density distributions of ^{12}Be, and the difference is obviously indicated in the surface structure of ^{12}Be. Inspired by this result, we bring forward a method to extract the ground state component of ^{12}Be.

In the method, we treat ^{12}Be as a system of ^{10}Be core plus two valence neutrons as usual. The ^{10}Be determines the nuclear-matter density distribution of the core part of ^{12}Be, while the two valence neutrons determine the outer part density distribution. According to the intruder configuration of ^{12}Be [4], the two valence neutrons are populated in $1p_{1/2}$, $1d_{5/2}$ and $2s_{1/2}$ states at certain occupation probabilities. So we can construct the outer structure of ^{12}Be according to a certain configuration as long as a model can give preferable density distribution of the two valence neutrons correspond-

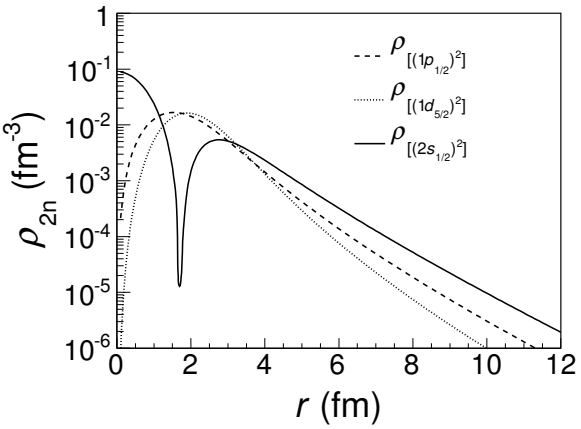

Fig. 7. Density distributions of the two valence neutrons corresponding to $1p_{1/2}$, $1d_{5/2}$ and $2s_{1/2}$ states.

ing to different states. By using an appropriate function to describe the core structure of ^{12}Be, we can construct a nuclear-matter density distribution of the ground state of ^{12}Be. By adjusting the proportion of the components, we can find a nuclear-matter density distribution which is consistent with the experimental result. Then the corresponding proportion can provide configuration information of ^{12}Be ground state.

We have tried to extract the ground state component of ^{12}Be in order to verify the feasibility of the method. As mentioned above, a precondition of the method is to obtain the valence neutron density distributions corresponding to $1p_{1/2}$, $1d_{5/2}$ and $2s_{1/2}$ states. Usually single particle model (SPM), three-body-model, cluster model, shell model, etc. are used to calculate the density distribution of the valence neutron. In this article, the SPM [35] is used. In this SPM, the Woods-Saxon potential, the Coulomb barrier and the centrifugal barrier are taken into account. The nuclear part of the potential assumed is written as

$$V=\left(-V_0+V_1(l\cdot s)\frac{r_{l\cdot s}^2}{r}\frac{\mathrm{d}}{\mathrm{d}r}\right)\left[1+\exp\left(\frac{r-R_c}{a}\right)\right]^{-1}, \tag{8}$$

where V_0 is the depth of the Woods-Saxon potential, $V_1 =$ 17 MeV is the $l\cdot s$ strength taken from Ref. [50], $r_{l\cdot s} = 1.1$ fm is the radius of spin-orbit potential, $R_c = r_0A^{1/3}$ ($r_0 =$ 1.2 fm) is the radius of the Woods-Saxon potential, and $a =$ 0.6 fm is the diffuseness parameter. V_0 is adjusted to reproduce the separation energy of the valence neutron. Here we treat the two valence neutrons as equal and set the separation energy of single valence neutron to be a half of the two-neutron separation energy of ^{12}Be. The corresponding nuclear-matter density distributions of the two valence neutrons are shown in Fig. 7. We can see that the $2s_{1/2}$ state has larger density in the surface. Although different models will not give exactly the same density distributions of the two valence neutrons, we infer that our result is less model-dependant based on the fact that s intruder valence neutron configuration is the chief cause of the halo-like structure in light nuclei just as the cases of ^{11}Li and ^{11}Be.

Then we consider a configuration mixing of $1p_{1/2}$, $1d_{5/2}$ and $2s_{1/2}$ for the two valence neutrons as follows:

$$\rho_{2n}^{n}=\alpha\rho_{[(1p_{1/2})^2]}+\beta\rho_{[(1d_{5/2})^2]}+(1-\alpha-\beta)\rho_{[(2s_{1/2})^2]}, \tag{9}$$

where α and β denote the occupation probability of $(1p_{1/2})^2$ and $(1d_{5/2})^2$ configuration, respectively. The integrals of the single configuration density and mixed density are all normalized to be two nucleons. Combining the ^{10}Be core distribution of Gaussian-Gaussian (GG) parametrzation given in Ref. [33], we calculated the corresponding σ_R and obtained a range of σ_R accordingly, as indicated in Fig. 8. We can see clearly that the σ_R is sensitive to the s orbital occupancy, and it is difficult to derive the p and d orbital occupancies from the σ_R data. This is because the $2s_{1/2}$ component contributes much more to the surface structure of ^{12}Be than the other components. By using the σ_I of ^{12}Be on C in Ref. [30], we extract the upper limit of the s orbital occupation probability to be about 56%. The upper limits are indicated by the vertical line in Fig. 8(c).

The result indicates that the s orbital is not a dominant component in ^{12}Be ground state. It is supposed to be the reason why the halo-like structure in ^{12}Be is not evident, because the s orbital component is the major contribution to the halo-like structure. Compared with the calculations given by Ref. [4, 20–22, 24], our result is relatively small (Table 3). Although our result is consistent with the β decay result given by Ref. [42], large uncertainty exists in both results. Therefore, higher precision extraction is needed.

By comparing the increasing trend of σ_R in insets (c) and (f) of Fig. 8, one can sees that at low energy region, σ_R is even more sensitive to the s orbital occupancy. This implies that the extraction uncertainty can be reduced if σ_R at low energy region is used. So, we calculate σ_R based on an s orbital occupation of 28% (half the value of the upper limit) and a p orbital occupation probability of 25%, as the percentage of $1p_{1/2}$ component was determined as $25 \pm 5\%$ [10]. The result is shown in Fig. 8(f), in which the hatched area indicates 2% error band. Thereby we can extracted that uncertainty of the s orbital occupation probability is about 23%. And take into account that six data points will be available from the experiment introduced in previous section, the precision of the extracted s orbital occupation probability is expected to be around 9%. This makes the experimental measurement of σ_R at low energy region more desirable.

Since the percentage of the $1p_{1/2}$ component has been determined by Gamow-Teller transition strengths [10], if either $1d_{5/2}$ or $2s_{1/2}$ component is extracted precisely, the ground state configuration of ^{12}Be shall be reliably determined. Our method provides a promising approach to extract the $2s_{1/2}$ component of ^{12}Be ground state and to determine the ground state configuration of ^{12}Be. Through the proposed σ_R measurements, we expect to extract the s orbital occupation probability with 9% uncertainty.

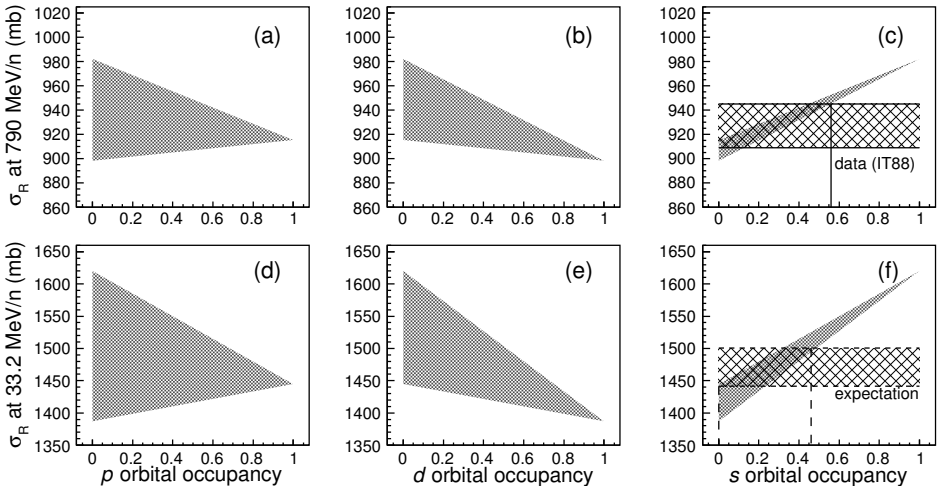

Fig. 8. The reaction cross section (σ_R) of ^{12}Be calculated at 33.2 MeV/nucleon and 790 MeV/nucleon, plotted against the occupation probability of the valence neutrons configuration in p, d and s orbit.

TABLE 3. Two-neutron occupancy (%) for ^{12}Be (g.s.) as ^{10}Be + 2n.

$(1p)^2$	$(1d)^2$	$(2s)^2$	Method	Ref.
38	29	32	Calc.	[20]
74	18	8	Calc.	[51]
32	15	53	Calc.	[21]
13-19	10-13	67-76	Calc.	[24]
31	34	35	Calc.	[22]
25			(^{3}He,^{6}He)	[52]
		20	β decay	[53]
35			β decay	[54]
50			β decay	[55]
		14-20	nucleon transfer reaction	[3]
32	30	38	extracted from spectroscopic factors	[4]
25 ± 5			extracted from Gamow-Teller Transition Strengths	[10]
		<56%	extracted from σ_I	present work

V. SUMMARY

In summary, the ground state structure of ^{12}Be is of great significance. The ambiguity of the configuration of ^{12}Be ground state has attracted our attention. We bring forward to determine the s orbital component of ^{12}Be ground state by measuring the σ_R of ^{12}Be on C and Al at several tens of MeV/nucleon. By using existed interaction cross section data of ^{12}Be on C at 790 MeV/nucleon, we roughly determine the upper limit of the s orbital occupation probability of ^{12}Be ground state to be 56% with SPM calculations. The precision of the s orbital occupation probability is expected to be 9% by using the proposed 2% σ_R data. The feasibility of the σ_R measurement is carefully studied and concrete procedures of the experiment are given.

ACKNOWLEDGEMENTS

We wish to thank Dr. Mitsunori Fukuda and his group in Osaka university for their precious help.

[1] Tanihata I, Hamagaki H, Hashimoto O, *et al*. Phys Rev Lett, 1985, **55**: 2676–2679.
[2] Freer M. Rep Prog Phys, 2007, **70**: 2149–2210.
[3] Kanungo R, Gallant A T, Uchida M, *et al*. Phys Lett B, 2010, **682**: 391–395.
[4] Navin A, Anthony D W, Aumann T, *et al*. Phys Rev Lett, 2000, **85**: 266–269.
[5] Ren Z Z and Xu G O. Phys Lett B, 1990, **252**: 311–313.
[6] Ren Z Z. J Phys G, 1994, **20**: 1185–1194.
[7] Ren Z Z, Xu G O, Chen B Q, *et al*. Phys Lett B, 1995, **351**: 11–17.
[8] Ren Z Z, Mittig M, Chen B Q, *et al*. Phys Rev C, 1995, **52**: R1764–R1767.
[9] Pain S D, Catford W N, Orr N A, *et al*. Phys Rev Lett, 2006,

96: 032502.
[10] Meharchand R, Zegers R G T, Brown B A, *et al*. Phys Rev Lett, 2012, **108**: 122501.
[11] Zahar M, Belbot M, Kolata J J, *et al*. Phys Rev C, 1993, **48**: R1484–R1487.
[12] Audi G, Wapstra A H, Thibault C. Nucl Phys A, 2003, **729**: 337–676.
[13] Kanada-En'yo Y and Horiuchi H. Progress of Theoretical Physics Supplement, 2001. 142(Copyright (c) Progress of Theoretical Physics 2001 All rights reserved.): pp. 205.
[14] Korsheninnikov A A, Aleksandrov D V, Aoi N, *et al*. Nucl Phys A, 1995, **588**: c23–c28.
[15] Freer M, Anglique J C, Axelsson L, *et al*. Phys Rev Lett, 1999, **82**: 1383–1386.
[16] Kanada-En'yo Y and Horiuchi H. Phys Rev C, 2003, **68**: 014319.
[17] Ito M, Itagaki N, Sakurai H. Phys Rev Lett, 2008, **100**: 182502.
[18] Dufour M, Descouvemont P, Nowacki F. Nucl Phys A, 2010, **836**: 242–255.
[19] Blanchon G, Vinh Mau N, Bonaccorso A, *et al*. Phys Rev C, 2010, **82**: 034313.
[20] Barker F C. J Phys G, 1976, **2**: L45–L47.
[21] Fortune H T and Sherr R. Phys Rev C, 2006, **74**: 024301.
[22] Barker F C. J Phys G, 2009, **36**: 038001.
[23] Fortune H T and Sherr R, J Phys G, 2009, **36**: 038002.
[24] Romero-Redondo C, Garrido E, Fedorov D V, *et al*. Phys Rev C, 2008, **77**: 054313.
[25] Glauber R J. Lectures in Theoretical Physics, Interscience, New York 1959, Vol. 1, pp. 315.
[26] Ma Y G, Shen W Q, Feng J, *et al*. Phys Lett B, 1988, **302**: 386–389.
[27] Ma Y G, Shen W Q, Feng J, *et al*. Phys Rev C, 1993, **48**: 850–856.
[28] Kox S, Gamp A, Perrin C, *et al*. Phys Rev C, 1987, **35**: 1678–1691.
[29] Shen W Q, Wang B, Feng J, *et al*. Nucl Phys A, 1989, **491**: 130–146.
[30] Tanihata I, Kobayashi T, Yamakawa O, *et al*. Phys Lett B, 1988, **206**: 592–596.
[31] Liatard E, Bruandet J F, Glasser F, *et al*. Europhys Lett, 1990, **13**: 401.
[32] Warner R E, McKinnon M H, Needleman J S. Phys Rev C, 2001, **64**: 044611.
[33] Ilieva S, Aksouh F, Alkhazov G D, *et al*. Nucl Phys A, 2012, **875**: 8–28.
[34] Takechi M, Fukuda M, Mihara M, *et al*. Phys Rev C, 2009, **79**: R061601.
[35] Tanaka K, Yamaguchi T, Suzuki T, *et al*. Phys Rev Lett, 2010, **104**: 062701.
[36] Tanaka K, Fukuda M, Mihara M, *et al*. Phys Rev C, 2010, **82**: 044309.
[37] Fan G W, Ph.D. thesis, Shanghai Institute of Applied Physics, Chinese Academy of Sciences, 2012.
[38] Takechi M, Fukuda M, Mihara M, *et al*. Eur Phys J A, 2005, **25**: 217–219.
[39] Ahlen S P. Phys Rev A, 1978, **17**: 1236–1239.
[40] Takechi M. Elucidation of the behavior of reaction cross sections at intermediate energies and halo structure of 6He. PhD Theis, Osaka University, 2006, 34–77.
[41] Bai X, Hu J. Phys Rev C, 1997, **56**: 1410–1417.
[42] Gangopadhyay G, Roy S. J Phys G Nucl Partic, 2005, **31**: 1111–1122.
[43] Tarasov O B and Bazin D. Nucl Phys A, 2004, **746**: 411–414.
[44] Sun Z, Zhan W L, Guo Z Y. Nucl Instrum Meth A, 2003, **503**: 496–503.
[45] Fang D Q, Shen W Q, Feng J, *et al*. Phys Rev C, 2000, **61**: 064311.
[46] Fang D Q, Shen W Q, Feng J, *et al*. Eur Phys J A, 2001, **12**: 335–339.
[47] Cai X Z, Zhang H Y, Shen W Q, *et al*. Phys Rev C, 2002, **65**: 024610.
[48] Zhang H Y, Shen W Q, Ren Z Z, *et al*. Nucl Phys A, 2002, **707**: 303–324.
[49] Ozawa A, Cai Y Z, Chen Z Q, *et al*. Nucl Instrum Meth B, 2006, **247**: 155–160.
[50] Bohr A and Mottelson B R, Nuclear Structure, Vol. I (Benjamin, New York, 1975).
[51] Thompson I J and Zhukov M V. Phys Rev C, 1996, **53**: 708–714.
[52] Robertson R G H. Atomic Masses and Fundamental Constants 5, Springer, 1976, pp. 147–153.
[53] Keller H, Anne R, Bazin D, *et al*. Z Phys A-Hadron Nucl, 1994, **348**: 61–62.
[54] Suzuki T and Otsuko T. Phys Rev C, 1997, **56**: 847–856.
[55] Barker F C. Phys Rev C, 1999, **59**: 535–538.